# Comparing IEC and WECC Generic Dynamic Models for Type 4 Wind Turbines

Martin Franke*, Adrien Guironnet†, and Carmen Cardozo†
* Grid Control and Grid Dynamics
Fraunhofer IEE, Kassel, Germany
martin.franke@iee.fraunhofer.de
† R&D - Power System Stability
RTE, La Défense, France
{adrien.guironnet, carmen.cardozo}@rte-france.com

***Abstract*—To ensure power system stability in the presence of a high penetration of power-electronic interfaced resources, Transmission System Operators (TSOs) require access to transparent, reliable and validated dynamic models to be able to conduct comprehensive large-scale studies. One possible approach is the utilization of so-called generic models that offer a modular structure capable of representing a wide range of installations by appropriately adjusting the parameters. This paper provides a thorough comparison of the two predominant generic models for Type 4 Wind Turbine (WT), developed by the International Electrotechnical Commission (IEC) and the Western Electric Coordinating Council (WECC), respectively. It highlights both the shared functionalities and the notable differences between these models, offering insights into their applicability. Furthermore, this analysis identifies unresolved questions regarding their implementation, emphasizing the need for further clarification to ensure a common understanding of their structure and consistent behavior across different tools.**

***Index Terms*—Generic Model, Power System Modeling, Power System Stability, WECC, IEC 61400-27, Wind Turbine, Type 4**

## I. Introduction

Transmission System Operators (TSOs) rely on accurate models and suitable simulation tools to assess the dynamic behavior of the power system and ensure its stability. However, as the share of distributed Inverter Based Generation (IBG) increases, TSOs face challenges in maintaining a realistic system representation. Creating ad-hoc dynamic models for each new installation is challenging, and thus, generic models have been proposed in the literature. These models offer a modular structure that can represent various installations by adjusting the parameters. Their modularity also favors readability and reusability.

For time domain positive sequence Root Mean Square (RMS) simulations typically used in large scale power system stability studies, there are two widespread sets of IBG generic models: one proposed by the International Electrotechnical Commission (IEC) standard 61400-27-1:2020 [1] and one developed by Western Electric Coordinating Council (WECC) [2] (hereafter referred to as IEC and WECC models, respectively).

This paper provides a comparison between the IEC and WECC models for Type 4 Wind Turbines (WTs), which are systems with full scale power-electronic converter connecting to the grid. While both models aim to represent the same technical systems and share many structural similarities, there are differences in implementation and parameter choices. Moreover, the equivalences between the models are not always obvious due to complex and compact signal flow diagrams. These features can lead to a lack of understanding of the practical implications of specific choices in terms of generality and accuracy offered by the models.

To cope with this issue, comparisons were already presented in [3], [4], [5] and [6]. However, they do not go as far into detail as this work or focused on Type 3 WT models. In addition, a new version of the IEC standard (in 2020) and new WECC models [7] have been released in the past years.

In this work, first, equivalent IEC and WECC model subsystems are identified and compared visually and logically. Second, equivalently parameterized models are simulated with Dynaωo, a hybrid Modelica/C++ open source simulation tool [8], using the models' implementations presented in [9] for IEC and [10] for WECC. Based on the results, the implications of model differences are documented. Finally, model improvements are proposed based on the analysis of documentation and performance assessment from both a dynamic and a numerical perspective.

The main contributions are thus:

1) A comparison and analysis of IEC and WECC Type 4 WT models including a common model structure.
2) A possible parameter mapping and/or translation between IEC and WECC frameworks.
3) A highlight on the models differences, supported by scenarios that illustrate their impact on the system variables.
4) A recommendation and possible solutions to handle an existing inconsistency in the WT reactive power control path of the IEC model.

The paper is structured as follows: Section II presents a structural comparison between the IEC and WECC models,

Submitted to the 23rd Power Systems Computation Conference (PSCC 2024).

highlighting first their equivalences and then their specificities on a common basis. Section III presents simulation results obtained with Dynaωo that illustrate the effects of those differences in the dynamic response of each model. Based on this analysis, Section IV provides a discussion on the expected behavior of generic models and issues recommendations to ensure proper implementation. Finally, conclusions are drawn in Section V.

## II. Comparison of Model Structure

### A. Description of standard models

The scope of this work is limited to the WT Type 4 models, i.e. the plant controller, which usually controls several WT on wind park level, is not included. Hence, the Power Collection System (PCS) that models the plant-internal grid (the elements between the WT terminal and the Point of Common Coupling (PCC) to the main grid) is also disregarded. In addition, we also neglect the IEC Electrical System Module that allows to represent passive elements, as series and ground impedances, between the Generator System (the converter) and the WT terminal since the WECC does not define those explicitly as part of the model. This choice's main implication is that the WT terminal, and therefore the measurement point for the WT control modules, is considered to be directly at the Generator System. It is important to point out that a clear and unambiguous definition of the measurement point is often missing in both the standards and the implementations leading to potential differences in results and analysis.

Furthermore, the protection system model is excluded from the comparison since the approach selected by each framework is fundamentally different: while IEC proposes generic modules, WECC recommends to use protection models that already exist in simulation software [11]. Finally, the two standard models have separate versions with and without a mechanical module that represents drive train oscillations (see Fig. 1). The mechanical modules are identical in IEC and WECC. They are not considered hereafter; this corresponds to model *Type 4A* in IEC and *Type 4B* in WECC, since their naming conventions are opposite. Although identical, the mechanical modules could augment minor differences of the other model parts and hence have been added for future work.

Having excluded the aforementioned model elements, the IEC and WECC models are structured as follows:

The 2020 IEC WT Type 4A model [1] includes a *Grid measurement module* (for control), a *Generator system module* and a *Generator control sub-structure* (with P control, Q control, current limitation and Q limitation modules).

The WECC WT Type 4B model [11] consists of the *REEC* (Renewable Energy Electrical Controls with P control, Q control and current limiting system), and the *REGC* (Renewable Energy Generator/Converter Model). As a starting point, the sub-models REGC_A and REEC_A were used.

### B. Development of Common Model Structure

For better comparability, both models have been put into one common generic structure which is based on the IEC model and can be seen in Fig. 1 and Fig. 2.

Tab. I shows how model parts have been re-assigned to the new common model structure. Different model parts have been merged together or separated from another. For example, for WECC, all measurement-related time delays in REEC have been moved to the common Wind Turbine Measurement Module (WT_meas), which does not exist in the original WECC model.

Further, a parameter and signal name mapping between IEC and WECC has been created and can be found in Appendix A (Tab. V). To facilitate the structural comparison, IEC names will be used in the common model structure when possible.

When referring to simulation model settings or to signals/-parameters that only apply to WECC, i.e. cannot be mapped to IEC, a `monospaced` font is used.

### C. Structural equivalences

In this section parallels between the two models are discussed based on the proposed common structure.

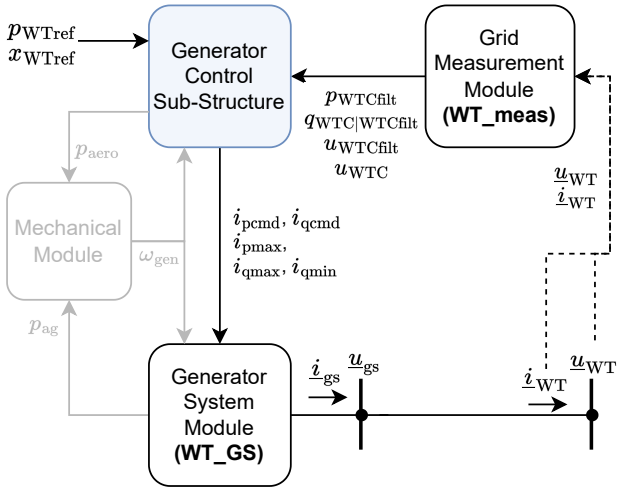


Fig. 1: Common generic structure of WT standard models.

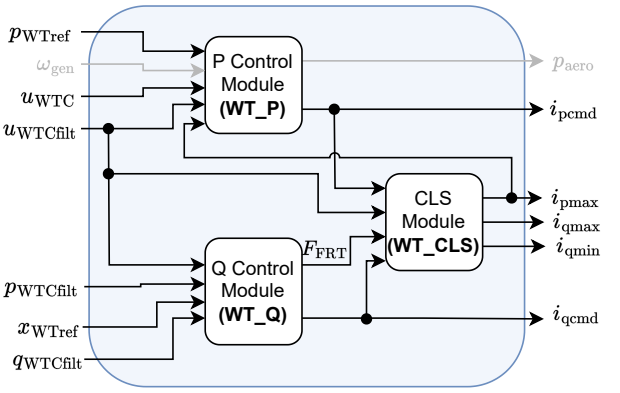


Fig. 2: Modules of generic Generator Control Sub-Structure.

TABLE I: Assignment of IEC and WECC model elements to common structure

| Common model structure module | Contains from IEC | Contains from WECC |
|---|---|---|
| P Control Module (WT_P) | P control module | P control path of REEC |
| Q Control Module (WT_Q) | Q control module, Q limitation module | Q control path of REEC |
| Current Limitation System Module (WT_CLS) | Current limitation module | Current Limit Logic of REEC |
| Grid Measurement Module (WT_meas) | Grid measurement module (for control) | Measurement filters of REEC |
| Generator System Module (WT_GS) | Generator system module | REGC, application of calculated current limits |

*1) WT_P:* Fig. 3 shows the Wind Turbine P Control Module (WT_P) with `MpUscale=0` (IEC) and `PFlag=0` (WECC). The model generates the active current command $i_{\mathrm{pcmd}}$ by dividing the filtered WT active power reference $p_{\mathrm{WTref}}$ by the measured voltage magnitude $u_{\mathrm{WTCfilt}}$. The dynamic response is dominated by the first order lag with time constant $T_{\mathrm{pord4A}}$.

*2) WT_Q:* The Wind Turbine Q Control Module (WT_Q) consists of a normal path and a fast reactive current injection path, which acts during and some time after an event (voltage drop or rise). There are multiple possible operating modes for each path, described in Tab. II and Tab. III. Fig. 4 and Fig. 5 show normal path mode 1 and fast injection path mode 1. Please note that $x_{\mathrm{WTref}}$ can be a voltage or reactive power set-point. In mode 1, the normal path consists of two cascaded Proportional-Integral (PI) controllers. The first one (reactive power controller) controls reactive power by generating a voltage reference for the second controller (voltage controller), which then generates the reactive current command $i_{\mathrm{qbasehook}}$. Input and output limitations are applied. During faults, the fast injection path adds an additional component to the q-axis

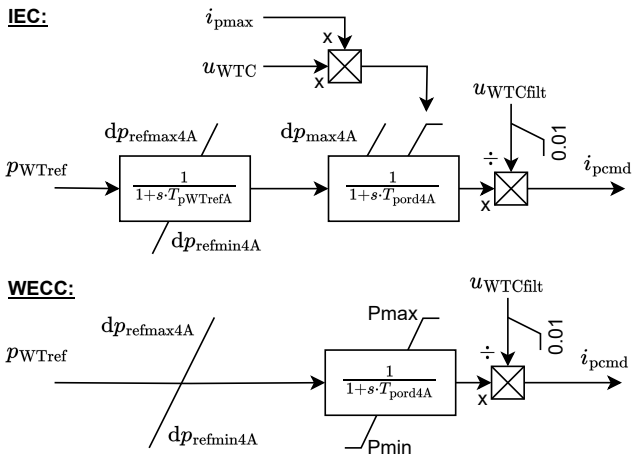


Fig. 3: Common module WT_P; mode 0

TABLE II: WT_Q normal path modes

| No. | Control Mode | WECC param. | IEC param. |
|---|---|---|---|
| 0 | U Control Mode | `QFlag=1, VFlag=0, PfFlag=0` | `M_qG = 0` |
| 1 | Q Control Mode | `QFlag=1, VFlag=1, PfFlag=0` | `M_qG = 1` |
| 2 | Q Control Mode (open loop) | `QFlag=0, VFlag=0/1, PfFlag=0` | `M_qG = 2` |
| 3 | PF Control Mode | `QFlag=1, VFlag=1, PfFlag=1` | `M_qG = 3` |
| 4 | PF Control Mode (open loop) | `QFlag=0, VFlag=0/1, PfFlag=1` | `M_qG = 4` |

TABLE III: WT_Q fast injection path modes

| No. | During Fault | Post Fault | IEC param. | WECC param. |
|---|---|---|---|---|
| 0 | $\Delta u$ droop | Same as during fault | `M_qFRT = 0` | - |
| 1 | Pre-fault $i_{\mathrm{qbasehook}}$ plus $\Delta u$ droop | Same as during fault | `M_qFRT = 1` | `Thld` $< 0$ |
| 2 | Like 1 | Pre-fault $i_{\mathrm{qbasehook}}$ plus constant | `M_qFRT = 2` | `Thld` $> 0$ |
| 3 | External injection (`i_dfhook`) | External injection (`i_pfhook`) | `M_qFRT = 3` | - |

current which is computed based on the voltage deviation $\Delta u$, a dead-band and droop (gain $K_{\mathrm{qv}}$).

In IEC, special attention must be paid to the reactive current signs as the documentation seems to be unclear or even inconsistent [1, Fig. 34]. In the fast injection path, $u_{\mathrm{WTC}}$ voltage drop leads to $\Delta u < 0$, resulting in $i_{\mathrm{qvhook}} < 0$. This behavior is opposite to the normal path. To react in the same sign convention as the normal path, $\Delta u$ should be $> 0$, resulting in $i_{\mathrm{qvhook}} > 0$. To solve this, the fast injection path's sign can be inverted, as has been done for the following simulations[1].

Another point worth mentioning is the dq sign convention. Positive $i_{\mathrm{qcmd}}$ is associated with capacitive reactive power in IEC. This is also the case in [12, Fig. 3.10]. In the dq-reference-frame definition of [13, Fig. 3.20], it is vice versa. Depending on the implemented sign conventions with the grid interface, a multiplication by -1 may also be needed in the Wind Turbine Generator System Module (WT_GS) module[1], as it is done in the WECC WT_GS, see Fig. 6.

*3) WT_CLS:* The Wind Turbine Current Limitation System Module (WT_CLS) acts after the WT_P and WT_Q controls.

[1]As a reference: In the DIgSILENT PowerFactory library model this is also done inside the fast injection path dead-band block / in the generator system model respectively.

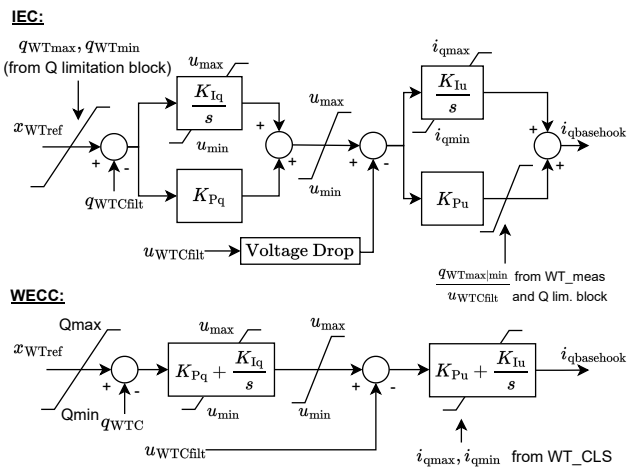


Fig. 4: Common module WT_Q (normal path); mode 1.

The priority between the active and reactive current is user-defined in both models. In addition to a maximum admissible current $i_{\max}$, Voltage Dependent Limits (VDL) can be defined for each current component through look-up tables such that $i_{\mathrm{p|qmax}} = \mathrm{i_{p|qmaxVDL}}(u_{\mathrm{WTCfilt}})$.

Appendix B shows python-inspired pseudocode comparing the current limitation algorithms.

*4) WT_meas:* The WT_meas contains all first order lag elements that represent measurement filters/delays. Measured quantities include the active and reactive power ($p_{\mathrm{WTC}}$ and $q_{\mathrm{WTC}}$), and the voltage $u_{\mathrm{WTC}}$ at the WT terminals. The index $_{\mathrm{WTCfilt}}$ is used to indicate filtered quantities.

*5) WT_GS:* In the WT_GS the converter is modeled as a current source[2]. It takes current commands from WT_P and WT_Q as well as limits from WT_CLS and injects the limited current ($\underline{i}_{\mathrm{gs}}$) into the network model. As illustrated in Fig. 6, the converter dynamics are modeled by a first order lag with a time constant $T_g$. Ramp rate limits are once more applied.

The purpose of the High-Voltage-Q-Management and Low-Voltage-P-Management blocks in the WECC model is to ensure numerical stability. In [11] an implementation is suggested, but it is also stated that every simulation software can have its own version. Hence, they will not be included in this comparison.

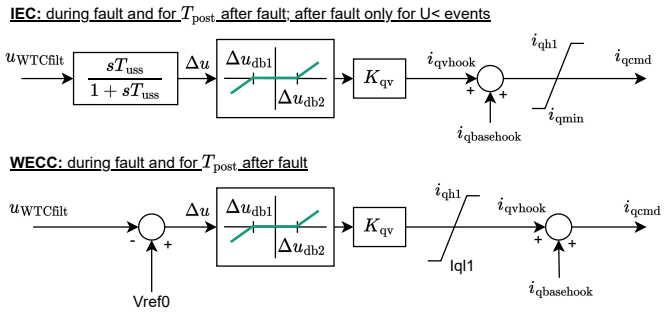


Fig. 5: Common module WT_Q (fast reactive current injection path); mode 1.

[2]WECC offers voltage-source models REGC_B and _C for weak networks, IEC does not.

## D. Structural specificities

In this section we describe a selection of model differences that either provide unique functionalities or lead to different behavior that cannot be reconciled by parametric settings.

*1) WT_P:* as illustrated in Fig. 3, the most visual difference between the IEC and WECC WT_P modules is the presence of an extra first order lag in series in IEC, as well as an additional positive rate limit ($dp_{\mathrm{max4A}}$). Furthermore, the WECC model allows to set minimum and maximum active power limits (`Pmin`, `Pmax`), which are fixed parameters, while the maximum active power in the IEC model is defined as the product of the maximal d-axis current ($i_{\mathrm{pmax}}$) and the unfiltered voltage $u_{\mathrm{WTC}}$, which are dynamic. Minimum power is often assumed to be zero. Finally, the IEC model has a low-voltage P scaling option (when `M_pUscale=1`) which further reduces the active power set-point during voltage dips.

*2) WT_Q – normal path:* as illustrated in Fig. 4, the IEC model includes a voltage drop compensation that allows to virtually displace the Point of Control (POC) of the voltage controller to account for passive elements between the POC and the point of measurement (if different). On the WECC side, this block has been added in the newer REEC_D version [14]. Secondly, the reactive power measurement is not filtered in WECC (see Fig. 4). Regarding limitations, IEC has a Q limitation module that can provide variable $q_{\mathrm{min|max}}$ limits

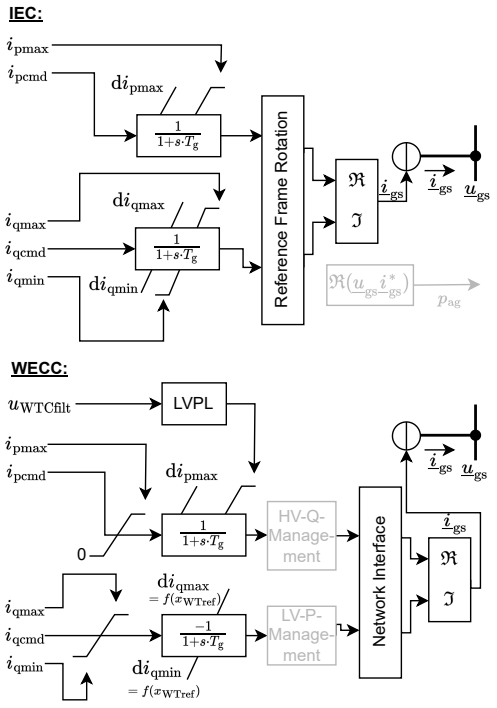


Fig. 6: Common module WT_GS.

TABLE IV: Elements that get frozen during FRT

| Element | IEC | WECC |
|---|---|---|
| WT_Q reactive power controller proportional part | | x |
| WT_Q reactive power controller integral part | x | x |
| WT_Q voltage controller proportional part | | x |
| WT_Q voltage controller integral part | x | x |
| WT_Q open-loop path $T_{\mathrm{qord}}$ lag | x | x |
| WT_Q open-loop path signal $i_{\mathrm{qbasehook}}$ | x | |
| Q Limitation Block inputs $u_{\mathrm{WTCfilt}}$ and $p_{\mathrm{WTCfilt}}$ | x | |
| WT_P $T_{\mathrm{pord}}$ lag | | x |

from look-up tables depending on voltage and active power, while WECC uses constant limits. Finally, during faults, when the Fault-Ride-Through (FRT) signal $F_{\mathrm{FRT}}$ is 1, the proportional gain of the voltage PI controller can be adapted in the IEC model (replacing $K_{\mathrm{Pu}}$ by $K_{\mathrm{PuFRT}}$ and removing its output limiter).

During FRT, $F_{\mathrm{FRT}}$ freezes certain model elements. A comparison of which elements are affected is shown in Tab. IV.

*3) WT_Q – fast injection path:* Fig. 5 shows that IEC and WECC propose different ways of calculating $\Delta u$, the measured voltage drop for fast reactive current response. The former considers a high pass filter with time constant $T_{\mathrm{uss}}$, while WECC considers the difference between the measurement and a reference voltage parameter `Vref0`. It is also worth noting that output limitations are not applied to the same signals: IEC limits the total $i_{\mathrm{qcmd}} = i_{\mathrm{qbasehook}} + i_{\mathrm{qvhook}}$ to $i_{\mathrm{qh1|qmin}}$. WECC limits $i_{\mathrm{qvhook}}$ to $i_{\mathrm{qh1|ql1}}$. Moreover, WECC uses the unfiltered voltage $u_{\mathrm{WTC}}$ for detecting voltage dips and activating FRT mode, which has been changed to the filtered value in the REEC_D version [14]. Finally, IEC defines the post-fault state ($F_{\mathrm{FRT}} = 2$) only in case of under-voltage events, while WECC defines it for over-voltage events as well.

*4) WT_CLS:* The IEC WT_CLS contains an additional high-voltage current limit logic ($K_{\mathrm{pqu}}$-logic) feature, which limits voltage-supporting reactive current injection during already high voltage. This is represented by K_pqulogic() in the code shown in Appendix B. In addition, during FRT, IEC introduces a separate maximum current value $i_{\mathrm{maxdip}}$. Furthermore, it is important to note that in IEC, outside FRT, P-Priority is always active, regardless of `M_qpri`. In WECC the time parameter `Thld2` exists, which holds the current limit $i_{\mathrm{pmax}}$ for a specified duration after fault clearing.

*5) WT_meas:* WECC does not consider any measurement filter for reactive power $q_{\mathrm{WTC}}$. No update on this regard has been reported in the more recent versions [14].

*6) WT_GS:* In IEC, limits for active and reactive power are applied to the output of a first-order lag with time constant $T_{\mathrm{g}}$. Conversely, in WECC the limits are applied before the lag element. Within WECC, the application of $\mathrm{d}i_{\mathrm{qmin|max}}$ depends on the sign of $x_{\mathrm{WTref}}$ [11, Fig. D-4]. Further, WECC incorporates a Low Voltage Power Limit (LVPL) look-up table, reducing maximum active power during low voltage. This has been removed in more recent versions, such as REGC_B. In IEC, there is a reference frame rotation block that includes a first-order lag applied to the phase angle to represent the Phase-Locked Loop (PLL).

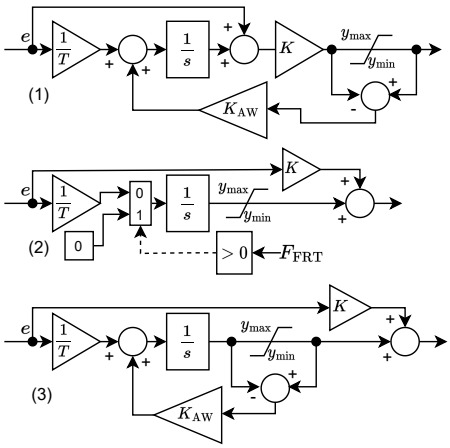


Fig. 7: PI Controllers with Anti-Windup: Dynaωo implementations for WECC (1) and IEC (2); Adapted implementation (3)

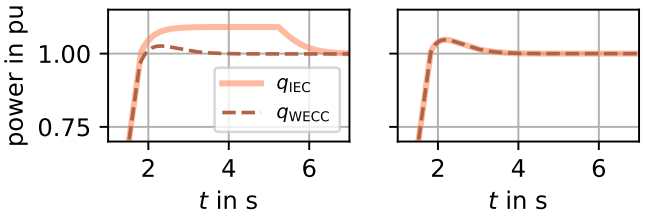


Fig. 8: Dynamic responses to reactive power step before (left) and after (right) adaption of Anti-Windup implementation.

## E. Discussion on implementation

When implementing the IEC or WECC models, developers need to make assumptions that influence the models' behaviors. Some noticeable aspects are mentioned in this section.

*1) Anti-Windup:* PI-controllers' Anti-Windup (AW) should be implemented when actuator limits are present. As recently discussed in [14], WECC did not use to specify the AW implementation. This changed in [2], where the reference AW suggested in [14] is recommended. Still, it is kept open to each vendor to adapt the implementation as necessary. In IEC [1, Fig. D.12] an AW integrator is specified, but its AW is only active during FRT. Also the implementation of the integrator limits is not specified. Hence, during implementation, suitable choices have to be made. Fig. 7 shows the resulting Dynaωo implementations for WECC (1) and IEC (2) respectively. The left side of Fig. 8 presents the response to a $1\,\mathrm{pu}$ reactive power step with those AW implementations. An adapted version that combines both implementations (Fig. 7 (3)) has been developed for both models to obtain equivalent behavior (right side of Fig. 8).

*2) PI Controller Output Limits:* Referring to Fig. 4 it can be seen that WECC does not specify whether to apply the PI controllers' limits ($u_{\mathrm{max|min}}$, $i_{\mathrm{qmax|qmin}}$) to the integral part or to the summed output of the controller. In this work it was assumed that the limits are applied to the integrators only, like in the IEC. This adaption is visible in Fig. 7.

*3) Limited first order lag:* The implementation of first order lag elements with output limitation is different in both models. The WECC standard does not specify how to implement limits into lag elements. In the Dynaωo implementation, for example, the limits are applied to the output signal, clipping it. The IEC specifies to integrate the limits into the lag element model in such a way that they are smoothly approached instead (see [1, Fig. D.6]). A resulting difference in dynamic response can be seen in the magnifying inset of Fig. 13, Section III.

## III. Simulation results

### A. Test case description

*1) Benchmark:* Fig. 9 shows the Single Machine Infinite Bus (SMIB) setup used.

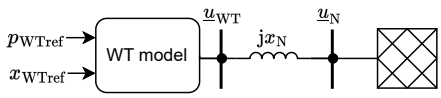


Fig. 9: Single line diagram of the test system.

*2) Scenarios:* A network impedance $x_{\mathrm{N}} = 0.1\,\mathrm{pu}$ is considered. The WT control modes are reactive power normal path mode 1 for Q steps and mode 0 for U steps (see Tab. II), fast injection path mode 1 (see Tab. III) and active power control without low-voltage active power scaling. The operating point is defined as follows: $p_{\mathrm{WTref}} = 1\,\mathrm{pu}$, $x_{\mathrm{WTref}} = 1\,\mathrm{pu}$ for the voltage in WT_Q normal path mode 0 and $x_{\mathrm{WTref}} = 0\,\mathrm{pu}$ for the reactive power in mode 1. The current limitation is set to reactive power priority. The full set of parameters is provided in Appendix C.

*3) Tests:*

- T1: an active power setpoint step (-0.5 pu)
- T2: a reactive power setpoint step (+0.3 pu)
- T3: a voltage setpoint step (+0.03 pu)
- T4: a solid fault at the WT terminal (150 ms)
- T5: a fault at the WT terminal (150 ms) with $x_{\mathrm{f}} = 0.2\,\mathrm{pu}$

*4) Output signals:* Variables will be displayed in per-unit with generation unit base and generated power is positive (producer reference frame). The measurement point is the WT terminal. The following variables will be shown: 1) active power and voltage/reactive power setpoints ($p_{\mathrm{WTref}}$, $x_{\mathrm{WTref}}$), 2) active and reactive power injected into the grid ($p_{\mathrm{IEC|WECC}}$, $q_{\mathrm{IEC|WECC}}$) and 3) voltage magnitude at WT terminal $u_{\mathrm{IEC|WECC}}$.

### B. Obtaining equivalent behaviour with both models

The parameters in Appendix C have been chosen to obtain similar model behaviors. If possible, specific functionalities have been deactivated by parameter settings.

*1) Reference tracking:* Fig. 10 and Fig. 11 show that the models behave the same for active and reactive power steps. Fig. 12 demonstrates that this is also the case for a voltage step.

*2) Solid fault:* In Fig. 13 the simulation of a solid fault at the WT terminal is shown. The results are largely overlapping. A difference can be seen in active power recovery in the upper graph, see Section II-E3.

### C. Emphasizing model differences and showcasing specific functionalities

In this section some model differences from II-D have been chosen and analyzed.

*1) Fast injection path voltage calculation:* Fig. 14 illustrates the impact of the different implementations of the fast reactive current injection described in Fig. 5. It shows a sustained voltage drop at $u_{\mathrm{N}}$. Even if it is not the most frequent, this scenario can be relevant. Indeed, according to German grid code [15] the WT has to stay connected up to 60 s at voltage levels above 0.85 pu. Because the IEC model uses a high-pass filter with time constant[3] $T_{\mathrm{uss}} = 30\,\mathrm{s}$ to determine $\Delta u$, the voltage difference decays over time, hence reducing fast current injection $i_{\mathrm{qvhook}}$ to 0, which reduces reactive

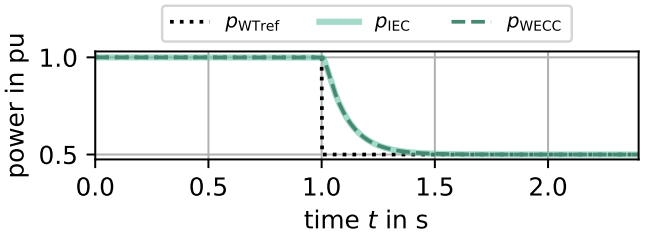


Fig. 10: T1 – active power ($p_{\mathrm{WTref}}$) step

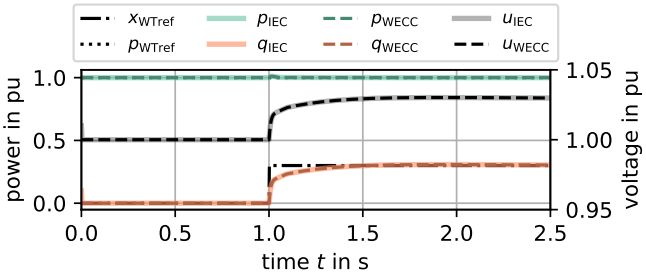


Fig. 11: T2 – reactive power ($x_{\mathrm{WTref}}$) step

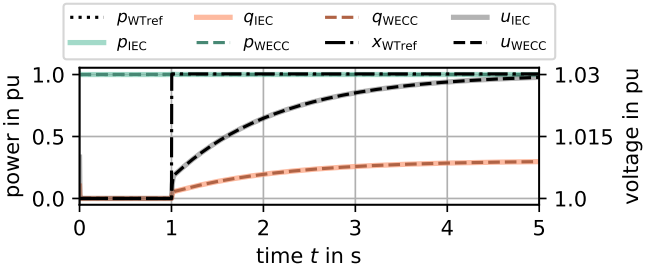


Fig. 12: T3 – voltage ($x_{\mathrm{WTref}}$) step

[3]Value as implemented in Dynaωo and DIgSILENT PowerFactory

current. In WECC, on the other hand, the voltage reference `Vref0` is static and the decay does not happen. To represent this behavior during long voltage drops, WECC would be more suitable or the IEC time constant $T_{\mathrm{uss}}$ has to be a very large value. The WECC implementation can, in turn, also lead to different behaviour if the pre-fault voltage is not `Vref0`, e.g. when two consecutive voltage drops occur.

*2) Active power dynamic response:* Fig. 15a shows the results for T5. There are obvious differences between the active power responses and those can be traced to mainly two structural model differences: the implementation of first order lags with limits (see Section II-E3) and the dynamic limit applied in IEC's WT_P as opposed to the constant limit parameter `Pmax` in WECC (see Fig. 3). Combined with the ramp rate limits the latter leads to a later return of active power.

When removing ramp rate limits and first order lag elements by setting the following parameters, the behavior becomes very similar, as shown in Fig. 15b. `rrpwr=di_pmax=100, T_g=Tg=1e-9, dp_max4A=100, T_pord4A=Tpord=1e-9`

However, these results are highly unrealistic, because dynamics are neglected and instantaneous responses enforced instead. Even in this case, differences remain in the response, originating from the dynamic versus constant active power limits as mentioned in Section II-D. $p_{\mathrm{WECC}}$ is shaped by the active current limit in WT_GS and $p_{\mathrm{IEC}}$ by the active power limit in WT_P.

*3) WT_CLS active/reactive power priority without FRT mode:* In Fig. 16 we can see a structural model difference. If the absolute current limit is reached after the reactive current step, the IEC WT_CLS prioritizes active power outside of FRT, although it is set to reactive power priority. This has also been described in [4].

*4) Reactive power measurement filter:* WECC does not have a measurement filter for reactive power. The effect of increasing the filter time constant $T_{\mathrm{qfilt}}$ on reactive power response in the IEC model can be seen in Fig. 17. It shows the moment of fault clearing for T4. The increased time constant introduces undershoot and damped oscillations.

*5) K_pqu-logic:* Fig. 18 shows the influence of IEC's $K_{\mathrm{pqu}}$-logic, as described in Section II-D4, on a voltage reference step response. Based on T3, the following parameters have been changed: `p_WTref=Pref=0, UpquMaxPu=1.1, M_qG=0, QFlag=1, VFlag=PfFlag=0`.

One can observe that for lower values of $K_{\mathrm{pqu}}$ the voltage is restricted to lower values as well. This is because the $K_{\mathrm{pqu}}$-logic limits capacitive reactive current during high voltage. This can be used to prevent already high voltages to be increased further.

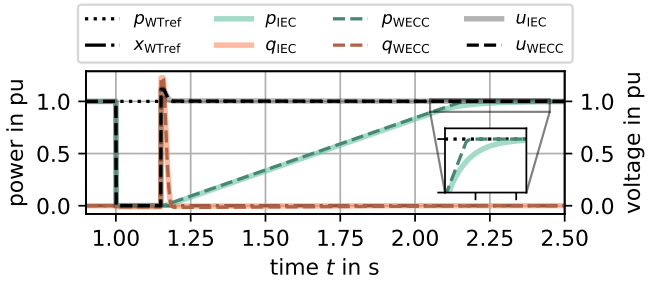


(a) fault and return of active power

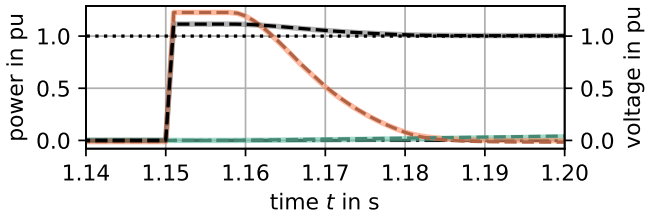


(b) close-up of fault clearing

Fig. 13: T4 – Solid short circuit for 150 ms

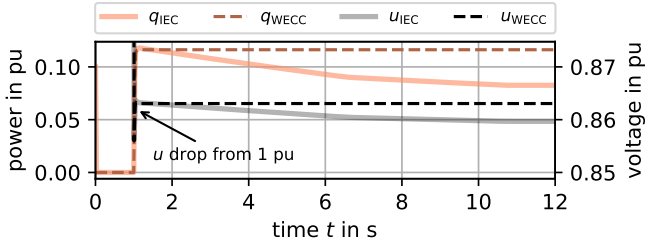


Fig. 14: Voltage drop with long duration

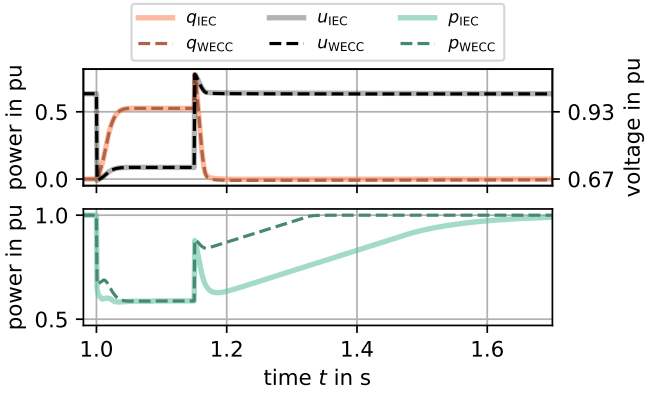


(a) parameterized according to Appendix C

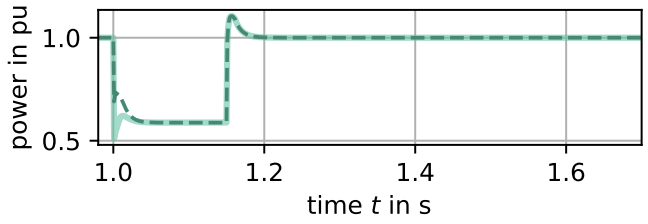


(b) re-parameterized for similar behavior (dynamics neglected)

Fig. 15: T5 – Short circuit for 150 ms with fault impedance

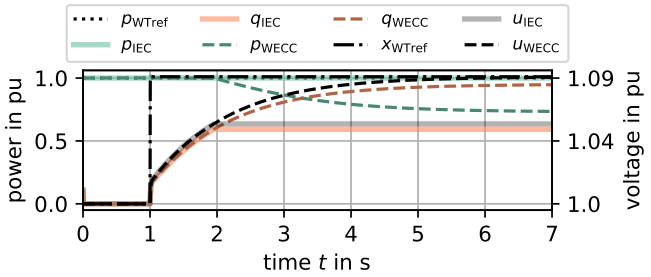


Fig. 16: Larger voltage setpoint step of +0.09 pu

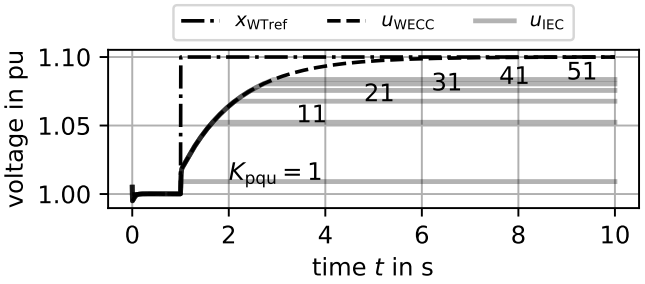


Fig. 18: Influence of IEC $K_{\text{pqu}}$-feature on voltage step response

## IV. Discussion and Recommendations

This work enables to show that WECC and IEC are lacking some important implementation details.

The authors recommend to add the following points to the WECC documentation: 1) PI controllers with separate proportional and integral parts, clarifying the limits' locations, 2) implementation of AW ideally in accordance with IEC [16], 3) implementation of limits of lag elements and 4) filter for measured reactive power.

On the IEC side, the standard would benefit from two modifications: 1) additional details on the AW integrator limits implementation, ideally in accordance with WECC [2] for comparability, and 2) fix of reactive current sign inconsistency between normal and fast injection path in WT_Q. One final remark concerning IEC is the absence of any voltage-source generator module, compared to WECC, which may be problematic for weak network studies.

## V. Conclusion and Future Work

This work presents an exhaustive comparison of the two most widely used generic Type 4 WT models: IEC and WECC [4]. The comparison is based on a common model structure, allowing for the identification of common features and highlighting the existing differences between the models. Simulations demonstrate that, with adapted parameters, similar behaviors can be achieved in most situations. However, in specific but realistic cases, notable differences become apparent.

Understanding these models' behaviors in different situations is valuable for large-scale stability studies and may help TSOs choosing the appropriate model for a certain type of stability study. For example, and even if the impact on large-scale systems still has to be formally assessed, one can deduce from Fig. 15a that the WECC model active power recovery after a fault will be faster compared to the IEC model and thus more optimistic regarding the associated frequency drop.

Additionally, this analysis identifies open questions regarding the proper implementation of both models, highlighting the impact of choices made by tool developers. These differences can lead to different behaviors in different tools, complicating the discussions between power system stakeholders. Recommendations for updates in the standard/documentation are provided.

Future work will focus on three aspects. Firstly, extending the analysis to include Wind Power Plant (WPP) controllers and/or the mechanical modules, which were not considered in this paper. Secondly, creating parameter sets consistent with the French grid code for use in planning studies of new installations. Finally, conducting larger system simulations to assess the impacts of model differences on stability criteria such as critical clearing time.

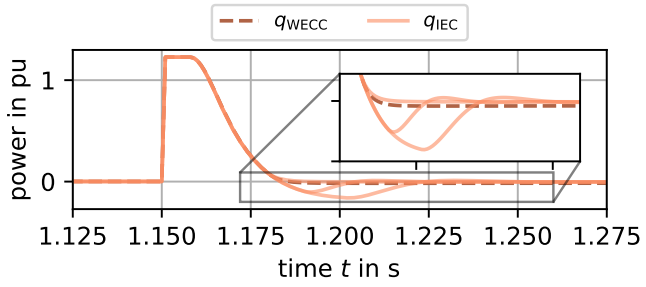


Fig. 17: Fault clearing of solid fault test T4 with IEC reactive power measurement filter $T_{\text{qfilt}} = [0, 0.008, 0.02]$ s.

[4]The Modelica models and the test cases used are available open source on github - https://github.com/dynawo/IEC-WECC-GenericModels-Comparison - while an extended report containing more analyses is available on arXiv.


## Acknowledgement

We acknowledge the support of our work by the German Ministry for Economy and Climate Protection and the funding agency Jülich within the project *LI-SA: assistance systems for secure operation of interconnected power systems with low inertia* (FKZ 03EI4059A). The authors are responsible for the content of this publication. This paper does not reflect the consolidated opinion of the project consortium *LI-SA*.


## References


[1] IEC, "IEC 61400-27-1 Wind Energy Generation Systems – Part27 – Electrical simulation models – Generic models," July 2020.

[2] EPRI, "Model User Guide for Generic Renewable Energy Systems (WECC)." https://www.epri.com/research/products/000000003002027129, Oct. 2023.

[3] A. Honrubia-Escribano, E. Gómez-Lázaro, J. Fortmann, P. Sørensen, and S. Martin-Martinez, "Generic dynamic wind turbine models for power system stability analysis: A comprehensive review," *Renewable and Sustainable Energy Reviews*, vol. 81, pp. 1939–1952, Jan. 2018.

[4] A. Lorenzo-Bonache, A. Honrubia-Escribano, J. Fortmann, and E. Gómez-Lázaro, "Generic Type 3 WT models: Comparison between IEC and WECC approaches," *IET Renewable Power Generation*, vol. 13, no. 7, pp. 1168–1178, 2019.
[5] I. Razzhivin, A. Suvorov, M. Andreev, and A. Askarov, "The comparison and analysis of Type 3 wind turbine models used for researching the stability of electric power systems," *International Journal of Emerging Electric Power Systems*, vol. 23, pp. 633–643, Aug. 2022.
[6] Ö. Göksu, P. Sørensen, J. Fortmann, A. Morales, S. Weigel, and P. Pourbeik, "Compatibility of IEC 61400-27-1 Ed 1 and WECC 2nd Generation Wind Turbine Models," in *Wind Integration Workshop*, 2016.
[7] WECC, "Approved Dynamic Model Library," tech. rep., WECC, Sept. 2022.
[8] A. Guironnet, M. Saugier, S. Petitrenaud, F. Xavier, and P. Panciatici, "Towards an Open-Source Solution using Modelica for Time-Domain Simulation of Power Systems," in *2018 IEEE PES Innovative Smart Grid Technologies Conference Europe (ISGT-Europe)*, pp. 1–6, Oct. 2018.
[9] B. Carbonell, C. Cardozo, Q. Cossart, T. Prevost, and G. Torresan, "An open source Modelica implementation of the IEC 61400-27-1 type 4 wind turbine model for power system stability assessment | Elsevier Enhanced Reader," 2022.
[10] M. Nuschke, S. Lohr, A. Guironnet, and M. Saugier, "Implementation and Validation of the Generic WECC Photovoltaics and Wind Turbine Generator Models in Modelica," *Modelica Conferences*, pp. 633–642, Sept. 2021.
[11] EPRI, "Model User Guide for Generic Renewable Energy System Models (WECC)," 2018.
[12] J. Machowski, Z. Lubosny, J. W. Bialek, and J. R. Bumby, *Power System Dynamics: Stability and Control, 3rd Edition*. Wiley, 2020.
[13] P. Kundur, *Power System Stability and Control*. New York: McGraw-Hill Education Ltd, Mar. 1994.
[14] P. Pourbeik, "Proposal For New Features For The Renewable Energy System Generic Models," Feb. 2023.
[15] VDE, "VDE-AR-N 4110 Anwendungsregel:2018-11 – Technische Regeln für den Anschluss von Kundenanlagen an das Mittelspannungsnetz und deren Betrieb," Nov. 2018.
[16] IEC, "DIN EN IEC 61970-302 – Schnittstelle für Anwendungsprogramme für Energiemanagementsysteme (EMSAPI) Teil 302: Allgemeines Informationsmodell (CIM) Dynamik," June 2023.

## APPENDIX A
## IEC AND WECC PARAMETERS MAPPINGS

TABLE V: Parameters and Signal Names Mapping

(a) WT_Q

| IEC | WECC |
|---|---|
| p:M_qG | p:Qflag, p:Vflag, p:PfFlag |
| p:M_qFRT | p:sign(Thld) |
| s:i_qbasehook | *s:Iqcmd_preinj* |
| p:K_Iu | p:Kvi |
| p:K_Pu | p:Kvp |
| p:K_PuFRT | - |
| p:i_qmax (WT_Q) | - |
| p:i_qmin (WT_Q) | - |
| p:u_max | p:Vmax |
| p:u_min | p:Vmin |
| s:u_ref0 | s:Vref1 |
| s:x_WTref | s:Qext |
| p:K_Iq | p:Kqi |
| p:K_Pq | p:Kqp |
| p:T_qord | p:Tiq |
| - | p:Qmax |
| - | p:Qmin |
| p:tan(phi_init) | p:tan(pfaref) |
| p:i_qh1 | p:Iqh1 |
| - | p:Iql1 |
| s:i_qcmd | *s:Iqcmd_prelim* |
| p:K_qv | p:Kqv |
| p:deltau_db1 | p:dbd1 |
| p:deltau_db2 | p:dbd2 |
| *s:deltau* | *s:deltau* |
| - | p:Vref0 |
| p:T_post | p:abs(Thld) |
| p:i_qpost | p:iqfrz |
| s:i_dfhook | - |
| s:i_pfhook | - |
| p:u_qdip | p:Vdip |
| p:u_qrise | p:Vup |
| s:F_FRT | s:Voltage_dip |

(b) WT_GS

| IEC | WECC |
|---|---|
| p:T_g | p:Tg |
| p:di_qmax | p:Iqrmax |
| p:di_qmin | p:Iqrmin |
| p:di_pmax | p:rrpwr |
| - | p:Lvplsw |
| - | p:Zerox |
| - | p:Brkpt |
| - | p:Lvpl1 |

(c) WT_P

| IEC | WECC |
|---|---|
| s:p_WTref | s:Pref |
| p:dp_refmax4A | p:dPmax |
| p:dp_refmin4A | p:dPmin |
| p:dp_refmax4B | p:dPmax |
| p:dp_refmin4B | p:dPmin |
| p:T_pWTrefA | - |
| p:T_pord4A | p:Tpord |
| p:T_pord4B | p:Tpord |
| - | p:Pmax |
| - | p:Pmin |
| s:i_pcmd | *s:Ipcmd_prelim* |
| p:dp_max4A | - |
| p:dp_max4B | - |
| p:u_pdip | - |
| p:T_Paero | - |
| s:p_aero | - |
| p:M_pUscale | - |
| - | p:PFlag |

(d) WT_CLS

| IEC | WECC |
|---|---|
| s:i_qmax | s:Iqmax |
| s:i_qmin | s:Iqmin |
| s:i_pmax | s:Ipmax |
| p:M_qpri | p:Pqflag |
| s:i_maxhook | - |
| s:i_qmaxhook | - |
| p:i_max | p:Imax |
| p:i_maxdip | - |
| p:i_pmax() | p:VDL2 |
| p:i_qmax() | p:VDL1 |
| p: K_pqu | - |
| p:u_pqumax | - |
| *s:i_maxset* | *s:i_maxset* |
| - | p:Thld2 |

(e) WT_meas

| IEC | WECC |
|---|---|
| s:u_WTCfilt | s:Vt_filt |
| s:q_WTCfilt | *s:Qgen_filt* |
| *s:q_WTC* | s:Qgen |
| s:p_WTCfilt | *s:Pe_filt* |
| s:u_WTC | s:Vt |
| p:T_pfilt | p:Tp |
| p:T_qfilt | - |
| p:T_ufilt | p:Trv |

(f) WT_Qlim

| IEC | WECC |
|---|---|
| s:q_WTmax | - |
| s:q_WTmin | - |

(g) Drive Train Model

| IEC | WECC |
|---|---|
| s:omega_WTR | s:omegat |
| s:omega_gen | s:omegag |
| s:P_aero | s:Pm |
| s:P_ag | s:Pe |
| p:k_drt | p:Kshaft |
| p:c_drt | p:Dshaft |
| p:H_WTR | p:Ht |
| p:H_gen | p:Hg |

(h) Legend

| symbol | meaning |
|---|---|
| s: / p: | signal/parameter |
| *italic* | not named in standard |
| - | not available |

## APPENDIX B
## CURRENT LIMITATION (PYTHON-INSPIRED PSEUDOCODE)

```
M_DFSLim, imax_hook, iqmax_hook = (0,0,0)
if F_FRT == 1:
    i_maxset = i_maxdip
else:
    i_maxset = i_max
# P Priority
if (M_qpri == 0) or (F_FRT == 0):
    i_pmax = i_pmaxVDL(u_WTCfilt)

    i_qlimit = min(
        i_qmaxVDL(u_WTCfilt),
        sqrt(max(0,
            i_maxset**2 - min(
                i_pcmd,
                i_pmaxVDL(u_WTCfilt))**2)
    ))
    i_qmin = -i_qlimit
    i_qmax = K_pqulogic(i_qlimit)
# Q Priority
else:
    i_qlimit = i_qmaxVDL(u_WTCfilt)

    i_qmin = -i_qlimit
    i_qmax = K_pqulogic(i_qlimit)
    i_pmax = min(
        i_pmaxVDL(u_WTCfilt),
        sqrt(max(0,
            i_maxset**2 - min(
                abs(i_qcmd),
                i_qmaxVDL(u_WTCfilt))**2)
    ))
```

(a) IEC

```
i_maxset = i_max
# P Priority
if Pqflag == 1:
    i_pmax = min(
        i_pmaxVDL(u_WTCfilt), i_maxset)
    i_qlimit = min(
        i_qmaxVDL(u_WTCfilt),
        sqrt(i_maxset**2 - i_pcmd**2)


    )
    i_qmin = -i_qlimit
    i_qmax = i_qlimit
# Q Priority
else:
    i_qlimit = min(
        i_qmaxVDL(u_WTCfilt), i_maxset)
    i_qmin = -i_qlimit
    i_qmax = i_qlimit
    i_pmax = min(
        i_pmaxVDL(u_WTCfilt),
        sqrt(i_maxset**2 - i_qcmd**2)


    )
```

(b) WECC

## APPENDIX C
## SIMULATION PARAMETERS

The following parameters are per-unit values if no unit is given.

### A. WECC Dynawo Model

SNom=100 MVA; RPu=0.0; XPu=0.0; VDLIp11, VDLIp12, VDLIp21, VDLIp22, VDLIp31, VDLIp32, VDLIp41, VDLIp42 = 0.9, 1.1, 1.1, 1.1, 1.11, 1.1, 1.12, 1.1; VDLIq11, VDLIq12, VDLIq21, VDLIq22, VDLIq31, VDLIq32, VDLIq41, VDLIq42 =0.9, 1.1, 1.1, 1.1, 1.11, 1.1, 1.12, 1.1; VRef1Pu=0.0; HoldIpMax=Thld2=0.0; **abs**(HoldIq)=**abs**(Thld)=0.1; sign(holdIq)=sign(Thld)=-1.0; IqFrzPu=0.0; PFlag=0.0; P0Pu=-1.0; Q0Pu=0.0; U0Pu=1.0; u0Pu=Complex(1,0); s0Pu=Complex(1,0); i0Pu=Complex(1,0); iInj0Pu=Complex(1,0); uInj0Pu=Complex(1, 0); UPhaseInj0=0.0; PInj0Pu=1.0; QInj0Pu=0.0; UInj0Pu=1.0; PF0=1.0; Id0Pu=1.0; Iq0Pu=0.0; Qflag, VFlag, PfFlag=1, 1, 0; Ppriority=Pqflag=1.0; UMinPu=Vdip=0.9; UMaxPu=Vup=1.1; Vref0Pu=1.0; Dbd1=-0.1; Dbd2=0.1; Kqv=2.0; Iqh1Pu=1.1; Iql1Pu=-1.1; Kqp=1.1; Kqi=2.25; VmaxPu=1.1; VminPu=0.9; Kvp=2.0; Kvi=10.0; Tiq=0.05 s; tPord=0.1 s; Dpmax=100.0; Dpmin=-100.0; IMaxPu=1.1; QMaxPu=0.4; QMinPu =-0.4; tG=0.007 s; tFilterGC=Tfltr=0.01 s; IqrMinPu=-100.0; IqrMaxPu=100.0; Rrpwr=1.0; RateFlag=0.0; Trv=0.01 s; tP =0.01 s;

### B. IEC Dynawo Model

Snom=100 MVA; ResPu=0.0; XesPu=0.0; GesPu=0.0; BesPu=0.0; TableIpMaxUwt=(straight line at i=1.1 p. u.); TableIqMaxUwt=(straight line at i=1.1 p. u.); URef0Pu=0.0; tPost=0.1 s; Mqfrt=1.0; IqPostPu=0.0; P0Pu=-1.0; PaG0Pu =1.0; Q0Pu=0.0; U0Pu=1.0; u0Pu=Complex(1,0); i0Pu=Complex(1,0); Mqg=1.0; Mqpri=0.0; Kpqu=20.0; UpquMaxPu=999.0; MdfsLim=false; UqDipPu=0.9; UqRisePu=1.1; DUdb1Pu=deltau_db1=-0.1; DUdb2Pu=deltau_db2=0.1; Kqv=2.0; IqH1Pu=1.1; IqMaxPu=1.1; IqMinPu=-1.1; Kpq=1.1; Kiq=2.25; UMaxPu=1.1; UMinPu=0.9; Kpufrt=2.0; Kpu=2.0; Kiu=10.0; tQord=0.05 s; tPOrdP4A=0.1 s; tPWTRef4A=1e-09 s; DPRefMax4APu=100.0; DPRefMin4APU=-100.0; DPMaxP4APu=1.0; IMaxPu=1.1; IMaxDipPu =1.1; QMaxPu=0.4; QMinPu=-0.4; QlConst=true; Kpaw=1000.0; MpUScale=false; UpDipPu=0.0; RDropPu=0.0; XDropPu=0.0; tUss=30 s; tG=0.007 s; DiqMinPu=-100.0; DiqMaxPu=100.0; DipMaxPu=1.0; Kipaw=100.0; Kiqaw=100.0; tUFilt=0.01 s; tPfilt =0.01 s; tQfilt=1e-09 s; tPll=1e-09 s; UPll1Pu=999.0; UPll2Pu=0.13;